

MULTI-SCALE DYNAMICS OF HIGH ENERGY THROUGHPUT SYSTEMS

Michael Baldea Prodromos Daoutidis

*Department of Chemical Engineering and Materials Science,
University of Minnesota, Minneapolis, MN 55455*

Abstract: The present paper analyzes the energy dynamics of process networks and/or staged processes whereby the material recycle streams interconnecting the units/stages take on the additional role of energy carriers. In the presence of large energy input and output flows, the networks considered are shown to exhibit a dynamic behavior with multiple time scales, with the variables in the energy balance evolving over a short time horizon, and the variables in the material balance exhibiting both fast and slow transients. A singular perturbation analysis is employed for the derivation of reduced order models for the fast and slow dynamics. Finally, an illustrative example and numerical simulation results are presented. Copyright 2007 IFAC

Keywords: process modeling, model reduction, process networks, high purity distillation

1. INTRODUCTION

Process integration (through material and energy recycle) is the rule rather than the exception in the process industries, leading to increased efficiency and lower capital costs. Improved economics come, however, at the cost of dynamic complexity: the presence of recycle streams introduces feedback interactions between the individual units, and gives rise to intricate, overall network dynamics (Hangos *et al.*, 1999; Pushpavanam and Kienle, 2001; Kiss *et al.*, 2002).

In our previous work (Kumar and Daoutidis, 2002; Baldea *et al.*, 2006), we have analyzed the material balance dynamics of several classes of networks with large material recycle streams. Using singular perturbation arguments, we demonstrated that their dynamic behavior exhibits several time scales. Also, we proposed a method for the derivation of reduced order

models describing the dynamics in the fast and slow time scale, and a hierarchical controller design framework which accounts for this time scale separation.

In the present paper, we focus on the energy dynamics of tightly integrated networks in which large energy flows are present and material recycle streams take on the additional role of energy carriers. Representative examples of such high energy throughput systems include high purity distillation columns, multiple effect evaporators (Seider *et al.*, 1999) and reactor-heat exchanger networks (Baldea and Daoutidis, 2006). We present a modeling framework that allows documenting rigorously that such networks exhibit a time scale separation both in the material and the energy dynamics. We describe a model reduction strategy based on a singular perturbation analysis, and highlight the control implications of this two time scale behavior. Finally, we illustrate the theoretical concepts with an example and numerical simulation results. Throughout our derivations, we use the standard order of magnitude notation $\mathcal{O}(\cdot)$.

¹ Financial support from the National Science Foundation, grant CTS-0234440, is gratefully acknowledged. MB was partially supported by a University of Minnesota Doctoral Dissertation Fellowship.

² MB currently with Praxair Technology Center, Tonawanda, NY. Contact email: daoutidi@cems.umn.edu

2. MODELING OF NETWORKS WITH HIGH ENERGY THROUGHPUT

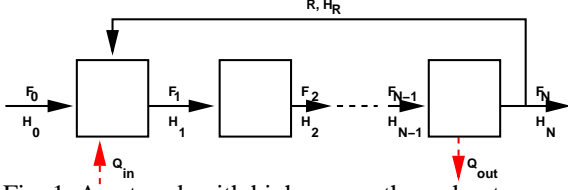


Fig. 1. A network with high energy throughput

We consider the network in Figure 1, consisting of N units/stages and a single material recycle stream. Let F_o denote the feed flowrate, F_i , $i = 1, \dots, N$ the outlet flowrate from the i th unit, R the recycle flowrate (with the associated specific energies H_i , $i = 1, \dots, N, R$) and let Q_{in} and Q_{out} be two energy flows (e.g., convective flow, heat generation by reaction or radiant heating) in and out of the network. Assuming that individual units are modeled as lumped parameter systems and that kinetic and potential energy contributions are negligible, the mathematical model that describes the energy balance of the network can be written in the form:

$$\begin{aligned} \dot{\theta}_1 &= F_o H_o + R H_r - F_1 H_1 + Q_{in} \\ &\vdots \\ \dot{\theta}_i &= F_{i-1} H_{i-1} - F_i H_i \\ &\vdots \\ \dot{\theta}_N &= F_{N-1} H_{N-1} - R H_r - F_N H_N - Q_{out} \end{aligned} \quad (1)$$

with θ_i being the enthalpies of units $i = 1, \dots, N$.

Equation 1 can be written in vector form as:

$$\dot{\theta} = \sum_{i=0, N} \gamma_i F_i H_i + \sum_{i=1}^{N-1} \gamma_i F_i H_i + \gamma_r R H_r + \gamma_q^{in} Q_{in} + \gamma_q^{out} Q_{out} \quad (2)$$

with $\theta = [\theta_1 \dots \theta_i \dots \theta_N]^T$ and γ_i, γ_q^j being appropriately defined vectors.

Let us now denote by $u_i = F_i/F_{i,s}$ and $u_r = R/R_s$ the dimensionless (possibly manipulated) inputs corresponding to the material flowrates, and define the ratios $k_i = F_{i,s}/R_s = \mathcal{O}(1)$, $i = 1 \dots N - 1$. We also consider that the recycle flowrate R is much larger than the network throughput, i.e., $F_{os}/R_s = \varepsilon_1 \ll 1$, where the subscript s denotes steady-state values. This feature is introduced for the sake of completeness (with respect to our previous work), although the main result of this work does not depend on it.

With the above notation, Equation 2 can be written as:

$$\dot{\theta} = \sum_{i=0, N} \gamma_i F_{i,s} u_i H_i + \frac{1}{\varepsilon_1} F_{os} \sum_{i=1}^{N-1} \gamma_i k_i u_i H_i + \frac{1}{\varepsilon_1} F_{os} \gamma_r u_r H_r + \gamma_q^{in} Q_{in} + \gamma_q^{out} Q_{out} \quad (3)$$

Using our previous results (Kumar and Daoutidis, 2002; Baldea et al., 2006) to explicitly capture the

stiffness due to the large recycle in the material balances, the overall model of the network becomes:

$$\begin{aligned} \dot{\mathbf{x}} &= \mathbf{f}(\mathbf{x}, \theta) + \sum_{i=0, N} \mathbf{g}_i(\mathbf{x}, \theta) u_i + \\ &\frac{1}{\varepsilon_1} \sum_{i=1}^{N-1} k_i \mathbf{g}_i(\mathbf{x}, \theta) u_i + \frac{1}{\varepsilon_1} \mathbf{g}_r(\mathbf{x}, \theta) u_r \\ \dot{\theta} &= \sum_{i=0, N} \gamma_i F_{i,s} u_i H_i + \frac{1}{\varepsilon_1} F_{os} \sum_{i=1}^{N-1} \gamma_i k_i u_i H_i + \\ &\frac{1}{\varepsilon_1} F_{os} \gamma_r u_r H_r + \gamma_q^{in} Q_{in} + \gamma_q^{out} Q_{out} \end{aligned} \quad (4)$$

with \mathbf{x} being the material balance variables.

Let us now concentrate on the energy dynamics of the system (4) and observe that the specific energies of the external and internal material flows, H_i , $i = 1, \dots, N$ and H_r can be expressed as a sum of two terms, an enthalpy term $e_i(\mathbf{x}, \theta)$ associated with the heat capacity of the stream, and an entropy-like term $s_i(\mathbf{x}, \theta)$ that captures (e.g., through the use of latent heats) any potential phase changes with respect to the phase of the feed stream F_o (typical are evaporation and condensation) occurring in the network. Specifically, we can write

$$H_i = e_i(\mathbf{x}, \theta) + s_i(\mathbf{x}, \theta)$$

Note that since the terms s_i denote a phase change with respect to the phase of the feed, we have $s_o = 0$. Furthermore, note that, in general, latent heats of vaporization are very high, and as such, the entropy-like terms will dominate the above sum, namely, we can write that (the dependence of e_i and s_i on \mathbf{x} and θ will be henceforth implied rather than explicitly denoted, for the sake of simplifying the notation):

$$\frac{e_i}{s_i} = \frac{1}{\nu_i} \varepsilon \ll 1$$

with $\nu_i = \mathcal{O}(1)$, $i = 1, \dots, N$.

Based on the above, and by denoting $\varepsilon_2 = \varepsilon \cdot \varepsilon_1$, the generic model (4) becomes:

$$\begin{aligned} \dot{\mathbf{x}} &= \mathbf{f}(\mathbf{x}, \theta) + \sum_{i=0, N} \mathbf{g}_i(\mathbf{x}, \theta) u_i \\ &+ \frac{1}{\varepsilon_1} \sum_{i=1}^{N-1} k_i \mathbf{g}_i(\mathbf{x}, \theta) u_i + \frac{1}{\varepsilon_1} \mathbf{g}_r(\mathbf{x}, \theta) u_r \\ \dot{\theta} &= \gamma_o(\mathbf{x}, \theta) F_{os} u_o e_o + \gamma_N F_{Ns} u_N e_N \left(1 + \frac{1}{\varepsilon} \nu_N\right) \\ &+ \frac{1}{\varepsilon_1} F_{os} k_i \left[\sum_{i=1}^{N-1} \gamma_i u_i e_i + \gamma_r u_r e_r \right] \\ &+ \frac{1}{\varepsilon_2} F_{os} k_i \left[\sum_{i=1}^{N-1} \gamma_i u_i e_i \nu_i + \gamma_r u_r e_r \nu_r \right] \\ &+ \gamma_q^{in} Q_{in} + \gamma_q^{out} Q_{out} \end{aligned} \quad (5)$$

We now make the following assumptions regarding the operation of the network:

- (1) The network material input and output streams are of the same phase. Equivalently, $s_N = 0$.

- (2) In order to supply the necessary heat for a phase change, the energy flows in and out of the network and the latent heat of the phase change of the internal streams are of comparable magnitude, *i.e.*,

$$Q_{in} = \frac{1}{\varepsilon_2} \omega_{in} \quad \text{and} \quad Q_{out} = \frac{1}{\varepsilon_2} \omega_{out}$$

with $\omega_{in} = \mathcal{O}(1)$ and $\omega_{out} = \mathcal{O}(1)$.

- (3) If no phase change occurs, the magnitude of the energy flows in and out of the network is similar to the energy flow corresponding to the internal material streams, *i.e.*,

$$Q_{in} = \frac{1}{\varepsilon_1} \omega_{in} \quad \text{and} \quad Q_{out} = \frac{1}{\varepsilon_1} \omega_{out}$$

Based on the above assumptions, an overall steady-state energy balance for the network indicates that the absolute values of the energy flows in and out of the network must be of comparable magnitude, *i.e.*, $|Q_{out,s}|/|Q_{in,s}| = k_q^* = \mathcal{O}(1)$. Also, according to the last two assumptions the network (4) has a high energy throughput, since in either of the assumed cases, the energy flow through the network due to the energy flows in and out of the network will be much larger than the energy flow associated with the small material input/output streams.

Under the above assumptions, the model of (4) becomes:

$$\begin{aligned} \dot{\mathbf{x}} &= \mathbf{f}(\mathbf{x}, \theta) + \sum_{i=0, N} \mathbf{g}_i(\mathbf{x}, \theta) u_i \\ &\quad + \frac{1}{\varepsilon_1} \sum_{i=1}^{N-1} k_i \mathbf{g}_i(\mathbf{x}, \theta) u_i + \frac{1}{\varepsilon_1} \mathbf{g}_r(\mathbf{x}, \theta) u_r \\ \dot{\theta} &= \gamma_o(\mathbf{x}, \theta) F_{os} u_o e_o + \gamma_N F_{Ns} u_N e_N \\ &\quad + \frac{1}{\varepsilon_1} F_{os} k_i \left[\sum_{i=1}^{N-1} \gamma_i u_i e_i + \gamma_r u_r e_r \right] \\ &\quad + \frac{1}{\varepsilon_2} F_{os} k_i \left[\sum_{i=1}^{N-1} \gamma_i u_i e_i \nu_i + \gamma_r u_r e_r \nu_r \right] \\ &\quad + \frac{1}{\varepsilon_2} [\gamma_q^{in} \omega_{in} + \gamma_q^{out} \omega_{out}] \end{aligned} \quad (6)$$

Thus, in what follows, we focus on systems with high energy throughput of the form of 6, or more generally, systems of the form :

$$\begin{aligned} \dot{\mathbf{x}} &= \mathbf{f}(\mathbf{x}, \theta) + \mathbf{G}^s(\mathbf{x}, \theta) \mathbf{u}^s + \frac{1}{\varepsilon_1} \mathbf{G}^l(\mathbf{x}, \theta) \mathbf{u}^l \\ \dot{\theta} &= \phi(\mathbf{x}, \theta) + \Gamma^s(\mathbf{x}, \theta) \mathbf{u}^s + \frac{1}{\varepsilon_1} \Gamma^l(\mathbf{x}, \theta) \mathbf{u}^l \\ &\quad + \frac{1}{\varepsilon_2} \hat{\Gamma}^l(\mathbf{x}, \theta) \mathbf{u}^l + \frac{1}{\varepsilon_2} \Gamma(\mathbf{x}, \theta) \omega \end{aligned} \quad (7)$$

with $\mathbf{x} \in \mathbb{R}^n$ denoting the vector of the state variables in the material balances and $\theta \in \mathbb{R}^N$ the vector of enthalpies. $\mathbf{u}^s \in \mathbb{R}^{m^s}$ is a vector of scaled input variables that correspond to the small material flowrates, $\mathbf{u}^l \in \mathbb{R}^{m^l}$ is a vector of scaled inputs corresponding to the large material flowrates, ω corresponds to the energy flows, \mathbf{f} and ϕ are vector functions and \mathbf{G}^s ,

\mathbf{G}^l , Γ^s , Γ^l , $\hat{\Gamma}^l$ and Γ are matrices of appropriate dimensions.

The model in Equation 7 includes *two* small singular perturbation parameters, ε_1 and ε_2 , which indicates a potential *three* time scale behavior for the dynamics of such networks. The rational approach for addressing the control of stiff, multiple time scale systems such as the one in Equation 7 involves the properly coordinated synthesis of separate fast and slow components of the control system, so that stability, output tracking and disturbance rejection can be obtained for the overall system. The design of such controllers and the closed-loop analysis should be performed on the basis of separate reduced-order models, that describe the dynamics in the fast and slow time scales. This is addressed in the section that follows.

3. NONLINEAR MODEL REDUCTION AND CONTROL

Note that $\varepsilon_2 = \varepsilon \cdot \varepsilon_1$ and hence $\varepsilon_2 \ll \varepsilon_1$. Thus, let us define the fast time scale $\tau_2 = t/\varepsilon_2$, and rewrite the model (7) in this fast time scale. Let us also consider the limit $\varepsilon_2 \rightarrow 0$, or, equivalently, the case of an infinitely high energy throughput. In this limit, we obtain:

$$\begin{aligned} \frac{d\mathbf{x}}{d\tau_2} &= 0 \\ \frac{d\theta}{d\tau_2} &= \hat{\Gamma}^l(\mathbf{x}, \theta) \mathbf{u}^l + \Gamma(\mathbf{x}, \theta) \omega \end{aligned} \quad (8)$$

which represents a description of the fast dynamics of the network, involving only the variables θ that pertain to the energy balance.

While the large internal material flowrates *do not affect* the total material holdup of the network or the holdup of any of the C components, the total enthalpy of the network *will be affected* by the large flows ω , and, therefore, it can be verified that the steady-state conditions that correspond to Equation 8 *are linearly independent*. Also, it is evident that the fast energy dynamics described by Equation 8 are only influenced by the large energy flows ω and by the flowrates of the large internal material streams, \mathbf{u}^l . The observations above indicate that upon setting ω (and possibly a subset $\mathbf{u}^l \setminus \hat{\mathbf{u}}^l$ of the large flow rates, with $\hat{\mathbf{u}}^l$ denoting the flow rates that are **not** set by feedback control³), by appropriate control laws, the Jacobian matrix

$$\frac{\partial}{\partial \theta} [\hat{\Gamma}^l(\mathbf{x}, \theta) \mathbf{u}^l + \Gamma(\mathbf{x}, \theta) \omega]$$

is nonsingular, and the equations $\mathbf{0} = \hat{\Gamma}^l(\mathbf{x}, \theta) \mathbf{u}^l + \Gamma(\mathbf{x}, \theta) \omega$ can be solved for the quasi-steady-state values $\theta^* = \mathbf{k}(\mathbf{x}, \hat{\mathbf{u}}^l)$ of the enthalpies (or temperatures)

³ Note in the sequel that the flow rates of the large material streams, \mathbf{u}^l are the only manipulated inputs available to control the fast component of the material balance dynamics, and hence only a **subset** of these inputs can and should be used to address control objectives related to the energy balance.

of each unit. Substituting the solution θ^* in the model (also accounting for the fact that only $\hat{\mathbf{u}}^l$ flowrates remain available after imposing the aforementioned control laws), we obtain a description of the dynamics of the network after the fast temperature ‘‘boundary layer’’

$$\begin{aligned}\dot{\mathbf{x}} &= \mathbf{f}(\mathbf{x}, \mathbf{k}(\mathbf{x}, \hat{\mathbf{u}}^l)) + \mathbf{G}^s(\mathbf{x}, \mathbf{k}(\mathbf{x}, \hat{\mathbf{u}}^l))\mathbf{u}^s \quad (9) \\ &\quad + \frac{1}{\varepsilon_1} \mathbf{G}^l(\mathbf{x}, \mathbf{k}(\mathbf{x}, \hat{\mathbf{u}}^l))\hat{\mathbf{u}}^l \\ \dot{\theta} &= \mathbf{0}\end{aligned}$$

or, after rearranging the model in order to group the available large and small flowrates,

$$\begin{aligned}\dot{\mathbf{x}} &= \tilde{\mathbf{f}}(\mathbf{x}) + \tilde{\mathbf{G}}^s(\mathbf{x})\mathbf{u}^s + \frac{1}{\varepsilon_1} \tilde{\mathbf{G}}^l(\mathbf{x})\hat{\mathbf{u}}^l \quad (10) \\ \dot{\theta} &= \mathbf{0}\end{aligned}$$

The model in Equation 10 is still stiff owing to the presence of flowrates of different magnitudes. Following a similar model reduction method it can be verified that the intermediate dynamics of the network, that evolve in the time scale $\tau_1 = t/\varepsilon_1$ will be of the form

$$\frac{d\mathbf{x}}{d\tau_1} = \tilde{\mathbf{G}}^l(\mathbf{x})\hat{\mathbf{u}}^l \quad (11)$$

and that the reduced-order model of the slow dynamics is described by a DAE system of the form:

$$\begin{aligned}\dot{\mathbf{x}} &= \tilde{\mathbf{f}}(\mathbf{x}) + \tilde{\mathbf{G}}^s(\mathbf{x})\mathbf{u}^s + \mathbf{B}(\mathbf{x})\mathbf{z} \quad (12) \\ \mathbf{0} &= \tilde{\mathbf{G}}^l(\mathbf{x})\hat{\mathbf{u}}^l\end{aligned}$$

Owing to the potential presence of three distinct scales in their dynamic behavior, the control of such networks should be addressed in a hierarchical manner. Energy-related control objectives are to be addressed in the fast time scale τ_2 , where ω and a subset of \mathbf{u}^l are available as manipulated inputs (Equation 8). Note that from an application point of view, the set of manipulated inputs in the fast time scale comprises oftentimes of only the large energy flows Q_i . Simple, distributed controllers for the stabilization (and fast disturbance rejection) of unit temperatures are a typical choice at this level. The control objectives in the intermediate time scale τ_1 (Equation 11) must be addressed using the large inputs $\hat{\mathbf{u}}^l$, as the inputs \mathbf{u}^s have no effect on the fast dynamics. These objectives include, *e.g.*, the stabilization of material holdups in the individual units, and can be addressed in a distributed fashion, typically using simple linear controllers. On the other hand, the slow dynamics that characterize the overall network behavior (*e.g.*, the evolution of product purity) are typically only driven by the small flowrates \mathbf{u}^s . Consequently, the objectives pertaining to the operation of the entire network are to be addressed in the slow time scale.

4. DYNAMICS OF HIGH PURITY DISTILLATION COLUMNS

High purity distillation columns are multi-staged separation systems that rely on a high internal recycle for

increasing the purity of the distillate/bottoms streams. The material balance dynamics was shown to exhibit a two-time scale behavior in (Kumar and Daoutidis, 2003). The present example aims to analyze the energy dynamics of such columns.

Consider a distillation column with N trays (numbered from top to bottom), to which a saturated liquid containing a mixture of two components (1 and 2) with mole fractions x_{1f}, x_{2f} , respectively, is fed at (molar) flowrate F_0 and temperature T_o on tray N_f . The heavy component 2 is removed at the bottom from the reboiler at a flowrate B , while the light component 1 is removed at the top from the condenser at a flowrate D . In this column, a large (compared to the feed, distillate and bottom product flowrates) vapor boilup V and liquid recycle R are used to attain a high purity of the products. We model the heat transfer in the reboiler and condenser by using heat duties and denote by Q_r and Q_c the heat duties in the reboiler and the condenser, respectively. We assume that the relative volatilities of the components are constant, and hence, that the phase equilibrium on tray i is given by: $y_{1,i} = \frac{\alpha_1 x_{1,i}}{1 + (\alpha_1 - 1)x_{1,i}}$. We consider that the heat capacities $C_{p,l}$ and $C_{p,v}$ of the liquid and vapor phases are constant. Under the above assumptions, a standard dynamic model of the column is obtained:

$$\begin{aligned}\dot{M}_C &= V - R - D \\ \dot{x}_{1,D} &= \frac{V}{M_C}(y_{1,1} - x_{1,D}) \\ \dot{T}_C &= \frac{1}{M_C C_{p,l}} [V(C_{p,v}T_1 + \sum_{j=1}^2 y_{j,1}\lambda_j - C_{p,l}T_C) - Q_C] \\ &\vdots \\ \dot{x}_{1,i} &= \frac{1}{M_i} [V(y_{1,i+1} - y_{1,i}) + R(x_{1,i-1} - x_{1,i})] \quad (13) \\ \dot{T}_i &= \frac{1}{M_i C_{p,l}} [V(C_{p,v}T_{i+1} + \sum_{j=1}^2 y_{j,i+1}\lambda_j) - V(C_{p,v}T_i \\ &\quad + \sum_{j=1}^2 y_{j,i}\lambda_j) + RC_{p,l}(T_{i-1} - T_i)] \\ &\vdots \\ \dot{x}_{1,N_f} &= \frac{1}{M_{N_f}} [V(y_{1,N_f+1} - y_{1,N_f}) + R(x_{1,N_f-1} - x_{1,N_f}) \\ &\quad + F(x_{1,N_f-1} - x_{1,N_f})] \\ \dot{T}_{N_f} &= \frac{1}{M_{N_f} C_{p,l}} [V(C_{p,v}T_{N_f+1} + \sum_{j=1}^2 y_{j,N_f+1}\lambda_j) \\ &\quad - V(C_{p,v}T_{N_f} + \sum_{j=1}^2 y_{j,N_f}\lambda_j) \\ &\quad + RC_{p,l}(T_{N_f-1} - T_{N_f}) + FC_{p,l}(T_o - T_{N_f})] \\ &\vdots \\ \dot{M}_B &= R - V + F - B \\ \dot{x}_{1,B} &= \frac{1}{M_B} [R(x_{1,N} - x_{1,B}) - V(y_{1,B} - x_{1,B}) \\ &\quad + F(x_{1,N} - x_{1,B})] \\ \dot{T}_B &= \frac{1}{M_B C_{p,l}} [RC_{p,l}(T_N - T_B) + FC_{p,l}(T_N - T_B) \\ &\quad + VC_{p,l}T_B - V(C_{p,v}T_B + \sum_{j=1}^2 y_{j,B}\lambda_j) + Q_B]\end{aligned}$$

where $M_C, x_{1,D}, y_{1,D}$, and T_C are the molar liquid holdup, liquid mole fraction, vapor mole fraction of component 1 and the temperature in the condenser, $M_i, x_{1,i}, y_{1,i}$ and T_i are the molar liquid holdup, liquid mole fractions, vapor mole fractions of component 1 and temperature on tray i and $M_B, x_{1,B}, y_{1,B}$, and T_B are the corresponding holdup, liquid mole fractions, vapor mole fractions and temperature in the reboiler and λ_j is the latent heat of vaporization of component j , $j = 1, 2$.

The presence of a large molar liquid recycle R implies an equally large molar vapor boilup V at the nominal steady state. On the other hand, the feed flow rate F , the distillate flow rate D and the bottom product flow rate B are of the same order of magnitude. Therefore, we can define $\varepsilon_1 = (F_s/R_s) \ll 1$ and $\kappa = V_s/R_s = \mathcal{O}(1)$, where the subscript s refers to the nominal steady state. Let us also define the scaled internal flowrates $\bar{V} = V/V_s$ and $\bar{R} = R/R_s$.

The latent heat of the vapor phase is typically very large, and the entropy-like term $C_{p,v} + \sum_{j=1}^2 y_j \frac{\lambda_j}{T}$ (with λ being the latent heat of vaporization) is much larger than the heat capacity of the liquid phase. Thus, e.g., for tray 1, we can write:

$$\frac{C_{p,l}}{\left(C_{p,v} + \sum_{j=1}^2 y_{j,1} \frac{\lambda_j}{T_1}\right)_s} = \varepsilon \ll 1$$

the index s again denoting steady-state values. By the same argument, a similar relation holds true for the other trays. In order to supply sufficient energy for the liquid phase to be vaporized, the energy input of the reboiler, Q_B , must be of the same order of magnitude as the energy flow associated with the vapor phase leaving the reboiler, that is

$$\frac{Q_{B,s}}{\left(\frac{1}{\varepsilon_1} F_s \kappa (C_{p,v} + \sum_{j=1}^2 y_{j,B} \frac{\lambda_j}{T_B})\right)_s} = \omega_B = \mathcal{O}(1)$$

Likewise, in order to condense the vapor phase in the condenser, its entire latent heat must be removed, and the condenser heat duty and the energy flow associated with the vapor phase leaving the first tray must be of similar magnitude:

$$\frac{Q_{C,s}}{\left(\frac{1}{\varepsilon_1} F_s \kappa (C_{p,v} + \sum_{j=1}^2 y_{j,1} \frac{\lambda_j}{T_1})\right)_s} = \omega_C = \mathcal{O}(1)$$

The evident implication of the above observations is that the amount of energy carried by the vapor stream from the bottoms of the column to the top is much larger than the amount of energy carried by the liquid reflux and, implicitly, than that carried by the streams F , D and B , and thus the column has a high energy throughput from the reboiler to the condenser. Let us now denote $\bar{Q}_C = Q_C/Q_{C,s}$ and $\bar{Q}_B = Q_B/Q_{B,s}$. With the above notation, the model of the distillation column can be put in the form of Equation 7. Details

of the modeling and model reduction procedure will be omitted for brevity.

For a simulation study we considered a distillation column for the separation of a mixture containing 80% (molar) normal-pentane (NP) and 20% 2-methyl butane (2MB), fed at a flowrate of 360 kmol/hr. It is desired that both distillation products be obtained at high purity (99.9% 2MB in the distillate and 99.9% NP in the bottoms). The column has 39 trays (the feed entering above tray 13) and is operated at atmospheric pressure. Trays are spaced at 0.7 m, the column is 1.5m in diameter and the weir height is 0.05m. The nominal distillate flowrate is 69.79 kmol/hr. The column was modeled with AspenPlus, using the rigorous `radfrac` column model, in conjunction with the Redlich-Kwong Soave equation of state for property estimation. Steady-state calculations indicated a reflux ratio of 87.67 (or, equivalently, a reflux rate 6119 kmol/hr). This is a consequence of the difficult separation problem posed by the two close-boiling components. Subsequently, we used Aspen Dynamics for time domain simulations. A basic control system was implemented with the sole purpose of stabilizing the (open-loop unstable) column dynamics. Specifically, the liquid levels in the reboiler and condenser are controlled using, respectively, the bottoms product flowrate and the distillate flowrate and two proportional controllers, while the total pressure in the column is controlled with the condenser heat duty and a PI controller. A controller for product purity was not implemented.

Dynamic simulations were aimed at capturing the multiple time scale behavior documented in the theoretical analysis presented above. Figures 2–4 show the evolution of the mole fraction of 2MB and of the temperature in the column reboiler and on selected column trays for a step rise in the heating agent flowrate in the reboiler. Notice that this change is equivalent to modifying the reboiler heat duty and, according to our analysis, acts upon the energy dynamics in the fast time scale. Indeed, as expected, the temperatures exhibit a fast transient in their behavior (with a subsequent slow approach to a new steady-state value), while the mole fractions (slow variables) only display a slow evolution towards the new steady state. Figure 6 shows the evolution of the temperature in the column reboiler and on the column trays for a step rise in the feed flowrate. According to our theory, this disturbance influences the slow material balance dynamics and has very little impact on the fast energy dynamics of the column. Indeed, the process parameters vary over a long time horizon. Moreover, the changes in the tray temperatures are small (Figure 6), as expected, confirming the analysis results.

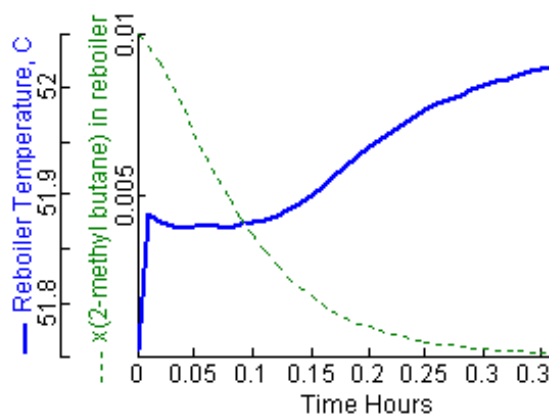


Fig. 2. Temperature and 2MB mole fraction in reboiler for a rise of the heating agent flowrate from 549630.0 kg/h to 600000 kg/h

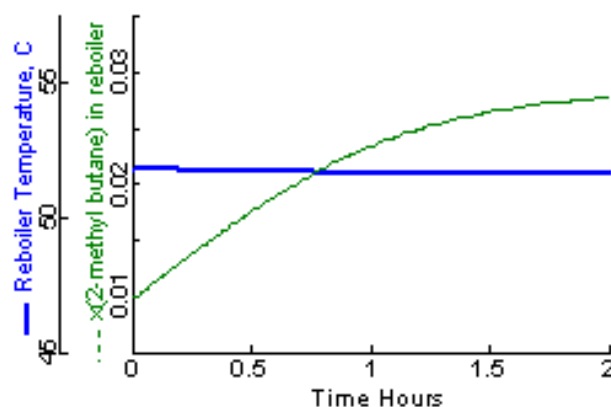


Fig. 5. Temperature and 2MB mole fraction in the reboiler for a rise of the feed flowrate from 360.0 kmol/h to 400 kmol/h

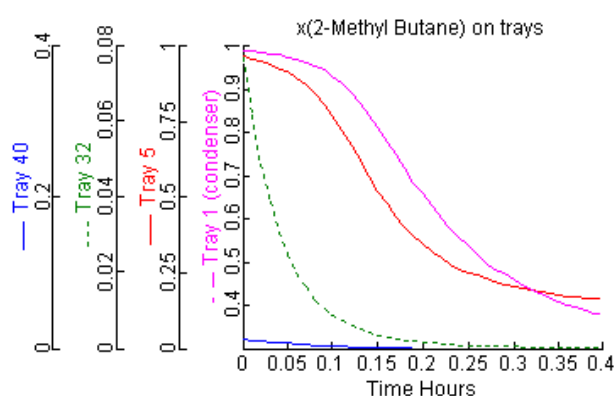


Fig. 3. 2MB mole fraction on the column trays for a rise of the heating agent flowrate from 549630.0 kg/h to 600000 kg/h

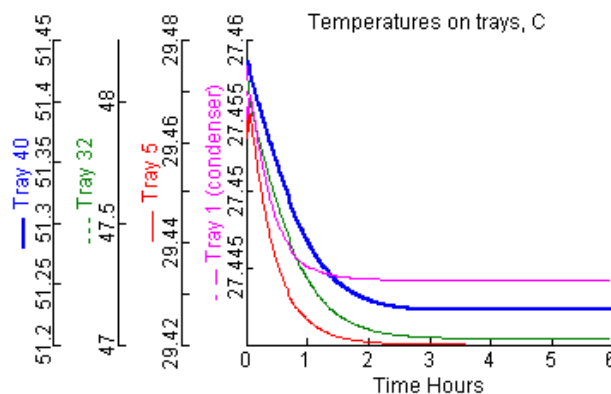


Fig. 6. Temperature on the column trays for a rise of the feed flowrate from 360.0 kmol/h to 400 kmol/h

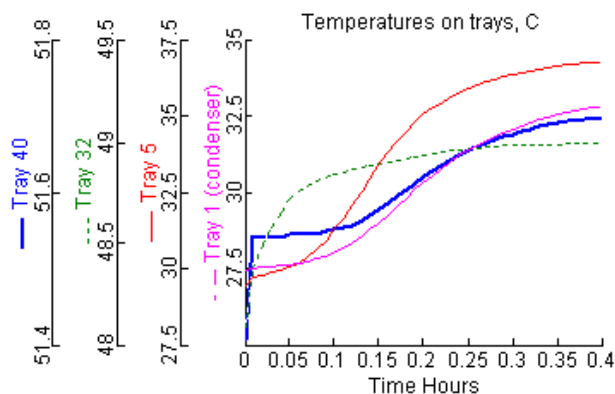


Fig. 4. Temperature on the column trays for a rise of the heating agent flowrate from 549630.0 kg/h to 600000 kg/h

REFERENCES

Baldea, M. and P. Daoutidis (2006). Model reduction and control of reactor-heat exchanger networks. *J. Proc. Contr.* **16**, 265–274.

Baldea, M., P. Daoutidis and A. Kumar (2006). Dynamics and control of integrated networks with purge streams. *AIChE J.* **52**, 1460–1472.

Hangos, K. M., A. A. Alonso, J. D. Perkins and B. E. Ydstie (1999). Thermodynamic approach to the

structural stability of process plants. *AIChE J.* **45**(4), 802–816.

Kiss, A.A., C.S. Bildea, A.C. Dimian and P. D. Iedema (2002). State multiplicity in CSTR-separator-recycle polymerization systems. *Chem. Eng. Sci.* **57**, 535–546.

Kumar, A. and P. Daoutidis (2002). Dynamics and control of process networks with recycle. *J. Proc. Contr.* **12**, 475–484.

Kumar, A. and P. Daoutidis (2003). Nonlinear model reduction and control for high-purity distillation columns. *Ind. Eng. Chem. Res.* **42**, 4495–4505.

Pushpavanam, S. and A. Kienle (2001). Nonlinear behavior of an ideal reactor separator network with mass recycle. *Chem. Eng. Sci.* **57**, 2837–2849.

Seider, W.D., J.D. Seader and D.R. Lewin (1999). *Process Design Principles*. John Wiley and Sons, Inc., New York.